MICROFRACTOGRAPHY OF TENSILE TESTS SURFACES OF WELDED JOINTS OF AUSTENITIC AND FERRITIC STEELS

B. NASIŁOWSKA [1], *Z. BOGDANOWICZ* [1], *J. FLĄDRO* [2], *M. NOGA* [3], *P. PASTUSZKA* [1], *B. SIERAKOWSKI* [1], *K. ZEGAR* [2]

[1] *Military University of Technology, Warsaw, Poland;*

[2] *Grupa Azoty PROREM Sp. z o.o., Tarnow, Poland;*

[3] *Zakłady Budowy Aparatury Chemicznej – Grupa Azoty w Tarnowie, Poland*

The results of microfractographic investigations of static tensile tests of welded joints of the 1.4539 austenitic and 1.4742 ferritic steels utilized for chemical installations production are presented. The tested types of steel resistant to corrosion indicate two different types of fracture. In the case of ferritic steel the brittle transcrystalline fracture at the boundaries of grains is observed, whereas, in the case of austenitic steel it is the plastic fracture.

Keywords: *ferritic steel, austenitic steel, microfractography.*

Fracture in plastic materials occurs when material strength is exceeded in the slip planes. In [1] metallurgical and mechanical properties of the automatic welding were examined based on AISI 904L stainless steel. Flux compound of 85% SiO_2 and 15% TiO_2 was used. Tensile fracture studies showed that the fracture occurred at the fusion zone for both weldments. Ductility was found to be greater for the flux-assisted weldments. This paper also investigates the structure–property relationships of the AISI 904L weldments using the combined techniques of optical and scanning electron microscopy.

The tensile fracture test was carried out and the yield strength and tensile strength of the joints were determined and their fracture surfaces were analyzed through scanning electron microscope [2]. Finally, the friction welding parameters were optimized the using particle swarm optimization technique. It was found that a complicated weld could be of the material could be easily obtained by the fusion welding process.

Nanoindentation experiments were conducted by using a Triboindenter instrumented nanoindenter (Hysitron, USA), which was calibrated on pure aluminum and silica as described in [3]. The result suggested a strong influence of the micromechanical incompatibility of the austenite phases on the texture evolution.

The available analysis of literature lacks a detailed comparative analysis of the micrography of static tensile welded joints of the 1.4539 and 1.4742 stainless steel operating in chemical installations.

The paper aim is to determine the properties of material, its crystallise structure as well as the purity and homogeneity based on the microfractography of welded joints of the 1.4539 austenitic and 1.4742 ferritic steels under static tensile testing.

Research object. Welded joints made of the 1.4539 austenitic steel with tungsten inert gas (TIG) welding method and the 1.4742 ferritic steel with metal active gas (MAG) welding method were subjected to comparative static tensile testing.

According to L. A. Schaffler, a weld structure after it is completely cooled down depends on the ratio of austenite-forming and ferrite-forming components [4, 5]. The considered types of corrosion – resistant steels differ in a content of austenite-forming and ferrite-forming components responsible for the ferrite area formation. The TIG and

Corresponding author: B. NASILOWSKA, e-mail: barbara.nasilowska@wat.edu.pl

MAG welds were made according to the same production technology as utilized in the company "Zakłady Budowy Aparatury Chemicznej – Grupa Azoty" in Tarnow. After edge rounding (V) a welding process through two passages from the face side was made, then the weld edge was undercut and pre-welded.

Structural analysis of metallographic microsections proved that a plane coagulation front with a gradual fusion of grain boundaries occurred in the weld made with the TIG method. A clearer growth of the grains near the fusion line in the heat affected zone (HAZ) occurred in the welded joint made of the 1.4742 ferritic steel compared to the joint made of the 1.4539 austenitic steel. In the heat-affected zone where the material did not undergo fusion fast fluctuations in temperature caused structural changes characterized by coarseness. The material of the weld, which underwent a total fusion during welding after transition into the solid state, was characterized by a dendritic structure in the pillar form perpendicularly oriented to the heat dissipation front.

Based on the tests results, mechanical properties of the 1.4539 austenitic and 1.4742 ferritic steels were determined with respect to the normative values (ultimate stress σ_u, see Table).

Test samples of dimensions of 170×30×5 mm with a 40 mm long gripping part were cut out with the Waterjet technique lengthwise with respect to the rolling direction.

Ultimate strength of the 1.4539 and 1.4742 steels

Steel	σ_u, MPa
1.4539 austenitic steel with TIG weld	589
1.4539 austenitic steel according to the PN-EN10027-1 standard	530…570
1.4742 ferritic steel with MAG weld	547
1.4742 ferritic steel according to the PN-EN10095 standard	500…700

Research results. Distributive fractures in the static tensile test of the considered 1.4539 steel welded joints occurred in the HAZ (Fig. 1*a*).Tests of metallographic microsections confirmed the presence of the recrystallization zone distant by 11 mm from the embedding line (Fig. 1*b*). This zone was characterized by a considerable grain fragmentation.

The biggest delaminating of the material observed on the fracture occurs in the middle of the fracture surface, which results from stress distribution in the neck and its surrounding. The greatest tensile stress caused by necking occurs in the middle of the fracture. The beginning of the fracture (fracture initiation) should be expected in the sample axis or in its surrounding. With necking the intensification of shear of the material layers in the direction of the most convenient slips occur until a distributive fracture is generated. Local shears of the material also prove its ability to considerable plastic strain in the analyzed welded joints (Fig. 2) [6].

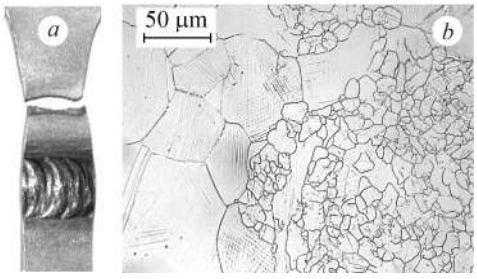

Fig. 1. Fracture (*a*) and recrystallization zone near the cracking line (*b*) obtained in a static tensile test of the 1.4539 steel welded joint made with the TIG method.

Fig. 2*e* shows the material delamination, with a visible texture resulted from hot rolling of the metal sheets in the central axis of the sample parallel to the rolling plane. The fractures were characterized by systems of cavities and protrusions creating a kind of plastic structure typical of plastic fracture (Fig. 2*a–d*). The intrusions occur-

red in loading and were caused by the material impurity after rolling (Fig. 2*b*–*d*). They enlarged due to plastic strain and plastic decohesion.

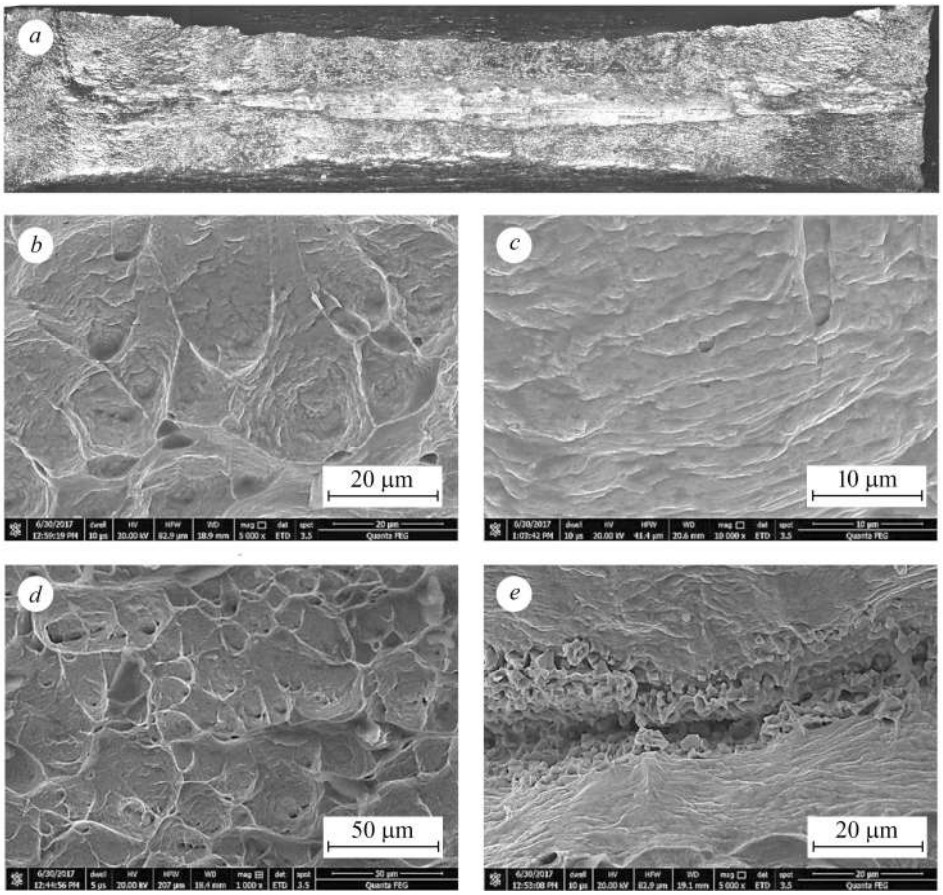

Fig. 2. Microstructure of a plane sample fracture of the 1.4539 austenitic steel welded joint obtained in a static tensile test (*a*–*c* – plastic cracking localized in the middle part of the breakthrough; *d* – localized in the axis of breakthrough; *e* – material delamination).

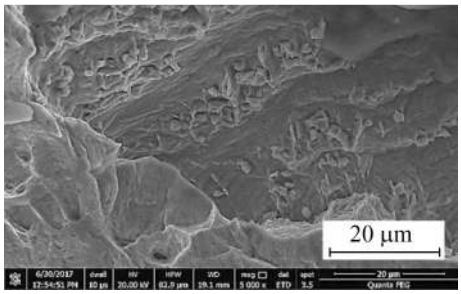

Fig. 3. Local mixed-mode fracture of the 1.4539 austenitic steel.

In the fracture surface outer areas a mixed-mode fracture was observed, i.e., sections of brittle and plastic scraps occurring alternately (Fig. 3).

Fracture surface of the 1.4742 ferritic steel joints welded with the MAG method was brittle (Figs. 4, 5) without clear signs of necking and perpendicular to the sample tensile axis. Numerous fissile fractures (Fig. 4*c*, *d*, Fig. 5*b*, *c*), intercrystalline fractures (Fig. 5*d*) and fractures at the grains boundaries (Fig. 5*a*) were observed. Fractures at the grain boundaries resulted from the lower material coherence, when the surface energy of the grains boundaries was lower than the energy in the cleavage planes [7].

Fracture occurred mainly in the planes typical of chromium (110), (112), and iron (100). Fractures in the cleavage planes (Fig. 5*c*) and secondary fractures (Fig. 5*d*) were also observed. Fig. 5 presents separation of the grain from the material structure. A clear

outline of the grain boundaries proves a harder structure of the inclusion which, due to the influence of ultimate strength on the sample, was separated in the whole.

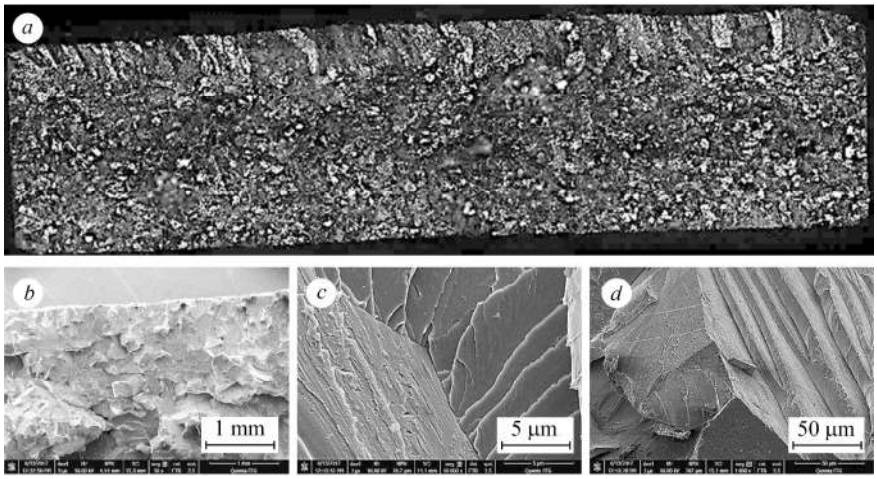

Fig. 4. Structure of fracture surface of the ferritic steel weld made with the MAG method (*a* – brittle transcrystalline fracture in the entire microfractographic breakthrough; *b* – brittle fracture located at the edge of the breakthrough; *c*, *d* – numerous fissile fractures).

In the final stage of fracture, in the grain boundaries zone, the plastic and brittle fractures were observed. Primary brittle fracture occurred along the transcrystalline planes and grain boundaries, and then local slips occurred at the tips and edges of the grains (Fig. 6). Minor numerous nucleating pins at the grain boundaries (indicated by arrow) were observed.

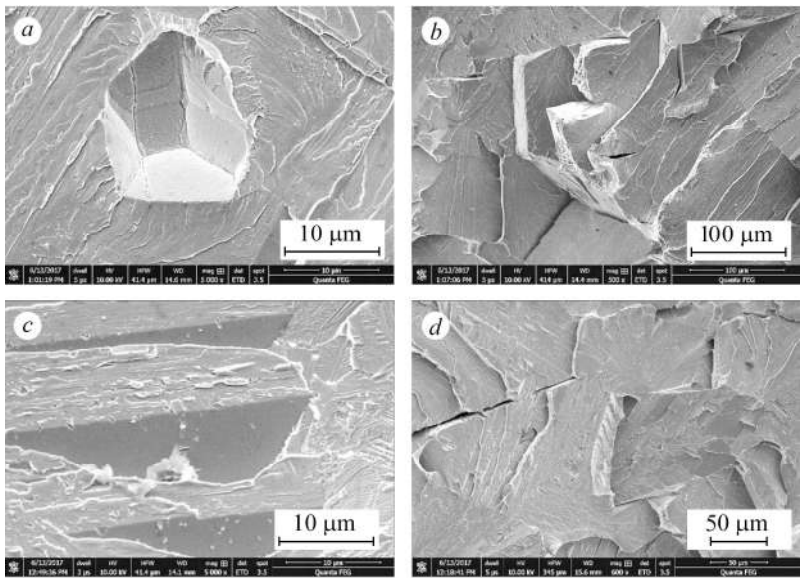

Fig. 5. Surface of brittle fracture at the 1.4742 ferritic steel grain boundary.

On the fractures surface the extrusions and intrusions on the metal edges were locally observed. A tendency to numerous intrusions in the 1.4539 austenitic steel has also noticed. In the 1.4742 ferritic steel a tendency to extrusion was observed, caused by the process of brittle and plastic fracture.

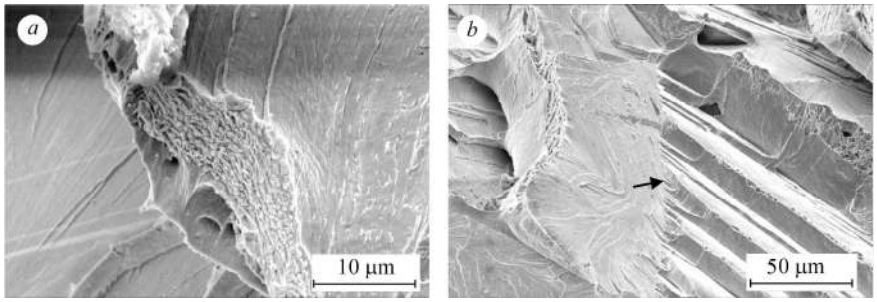

Fig. 6. Surface of brittle fracture at the 1.4742 steel grain boundary with the edges rounding.

CONCLUSIONS

The results of microfractographic static tensile fracture test of the welded joints of the 1.4539 austenitic steel made with TIG method and of the 1.4742 ferritic steel made with the MAG method allow us to draw the following conclusions: static tensile fracture test for the considered welded joint showed the final cracking of welding joints, which occurred outside the weld itself. The termination was registered in the HAZ area but at the border of the recrystallization zone; joints made of the 1.4539 austenitic steel were characterized by plastic fracture, whereas, in the case of the 1.4742 ferritic steel brittle fracture was observed mainly at the grains boundaries; tensile ultimate strength was 547 MPa for the 1.4742 steel and 589 MPa for the 1.4539 steel. The difference in strength is caused by, among others, various fracture mechanisms occurring in these joints.

РЕЗЮМЕ. Подано результати мікрофрактографічних досліджень, зруйнованих розтягом зразків зі зварними з'єднаннями корозійнотривких аустенітної 1.4539 та феритної 1.4742 сталей, що використовуються для виробництва хімічних установок. Сталі різної мікроструктури руйнуються за різними механізмами: якщо аустенітній сталі властиве пластичне руйнування, то феритній – крихке та крізьзеренне.

РЕЗЮМЕ. Представлены результаты микрофрактографических исследований, разрушенных растяжением образцов со сварными соединениями корозийностойких аустенитной 1.4539 и ферритной 1.4742 сталей, используемых для производства химических установок. Стали различной микроструктуры разрушаются разными механизмами: если аустенитной стали свойственно пластическое разрушение, то ферритной – хрупкое и сквозьзеренное.

1. *Effect* of autogeneous GTA welding with and without flux addition on the microstructure and mechanical properties of AISI 904L joints / K. D. Ramkumar, J. L. N. Varma, G. Chaitanya, A. Choudhary, N. Arivazhagan, and S. Narayanan // Mat. Sci. & Eng. – 2015. – **636**. – P. 1–9.
2. *Artificial* neural network simulation and particle swarm optimisation of friction welding parameters of 904L superaustenitic stainless steel / K. Balamurugan, A. P. Abhilash, P. Sathiya, and S. A. Naveen // Multidiscipline Model. in Mat. and Struct. – 2014. – **10. 2**. – P. 250–264.
3. *Effect* of shielding gases on microstructure and mechanical properties of super austenitic stainless steel by hybrid welding / P. Sathiya, M. Mishra, B. Shanmugarajan // Mat. Des. – 2012. – **33**. – P. 203–212.
4. *Castro R., and Cadenet J. J.* Metalurgia spawania stali odpornych na korozję i żarowytrzymałych // WNT. – Warsaw. – 2016. –**111–112**. – P. 22–25.
5. *Effects* of filler metals on the segregation, mechanical properties and hot corrosion behaviour of pulsed current gas tungsten arc welded super-austenitic stainless steel / K. D. Ramkumar, A. Chandrasekhar, A. Srivastava, H. Preyas, S. Chandra, S. Dev, and N. Arivazhagan // J. Manufact. Proc. – 2016. – **24**. – P. 46–61.
6. *Bogdanowicz Z., Jóźwik P., Nasiłowska B.* Microstructure and mechanical behavior of a CO_2 laser and TIG welded 904L steel // Metallurgy and Foundry Eng. – 2014. – **40. 2**. – P. 69–81.
7. *Effects* of normalizing processes on microstructure and impact toughness in Ti-bearing weld metal of multilayer MAG welded HSLA steel / S. Lu, X. Wang, W. Dong, and Y. Li // ISIJ Int. – 2013. – **53. 1**. – P. 96–101.

Received 21.11.2017